Volume 58
Number 88
14 November 2022
Pages 12251–12374

ChemComm

Chemical Communications

rsc.li/chemcomm

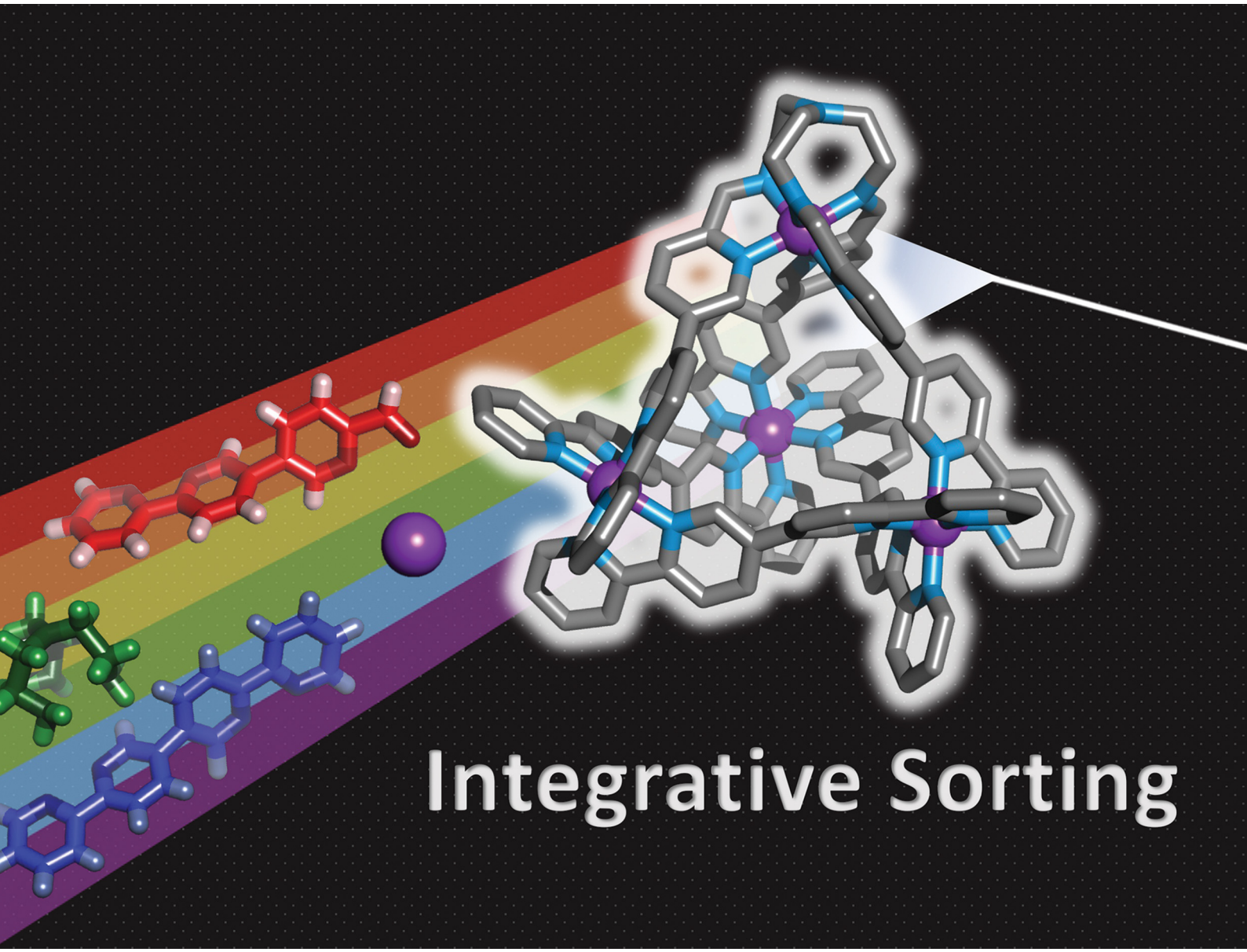

ISSN 1359-7345

ROYAL SOCIETY OF CHEMISTRY

COMMUNICATION

Imogen A. Riddell *et al.*

Synthesis and characterisation of an integratively self-sorted $[Fe_4L_6]^{8+}$ tetrahedron

ChemComm

COMMUNICATION

View Article Online
View Journal | View Issue

Check for updates

Cite this: *Chem. Commun.*, 2022, **58**, 12301

Received 19th August 2022,
Accepted 10th October 2022

DOI: 10.1039/d2cc04624e

rsc.li/chemcomm

Open Access Article. Published on 18 2022. Downloaded on 2.10.2024 . 19:22:38.
This article is licensed under a Creative Commons Attribution 3.0 Unported Licence.

Synthesis and characterisation of an integratively self-sorted $[Fe_4L_6]^{8+}$ tetrahedron†

Lauren L. K. Taylor, Rebecca Andrews, April C. Y. Sung, Iñigo J. Vitorica-Yrezabal and Imogen A. Riddell *

Isolating metal–organic cage structures which incorporate more than one distinct ligand has been challenging due to competing pressures from narcissistic and social sorting phenomena. Here we report the first example of exclusive formation of a single tetrahedral product from a reaction mixture containing two different bidentate ligands. Exclusive formation of the tetrahedron, which incorporates one unique metal vertex, relies on a triamine to orientate the heteroditopic ligand. Inclusion of perchlorate counterions during the self-assembly process is also found to be a requirement if social sorting is to be avoided. The C_3-symmetric structure is characterised by HR-MS, NMR spectroscopy and X-ray crystallography, and provides proof of principle for use of heteroditopic ligands in classical M_4L_6 supramolecular structures, opening exciting possibilities for their use in separation, storage and catalysis applications.

Within a subcomponent mixture, self-sorting principles can control the spontaneous self-assembly process and promote the formation of specific products.[1,2] This phenomenon is prevalent throughout nature, governing processes such as base pairing in DNA,[3] the self-fractioning of white blood cells in human blood[4] and the highly-ordered, spontaneous grouping of alike neurons during foetal brain development.[5] Recently there has been a growing interest in understanding and controlling complex self-sorting phenomenon in synthetic systems.[6–12] In the field of metallo-supramolecular architectures the desire to controllably generate complex structures with unusual and useful functionality has led researchers to explore incorporation of reduced symmetry ligands[13–17] as well as the formation of heteroleptic structures.[18–24] Generation of discrete structures from these components requires that ligands are controllably orientated through sorting phenomena.

Self-sorting processes have been defined as either narcissistic or integrative,[25,26] where narcissistic self-sorting describes the phenomenon of self-association[2,27] and integrative self-sorting describes the combination of multiple different structural components within a single system.[11,27] Commonly these terms are applied to the self-assembly of complexes from more than one homoditopic ligand, however, the self-assembly of reduced symmetry heteroditopic ligands can also be defined using these descriptors. In the latter case it is the coordination environment around the metal ion that is considered.[7,11] For systems where neither narcissistic nor integrative sorting dominates, it is also possible to generate equilibrium mixtures containing several thermodynamic products of similar energies. This socially sorted mixture is termed a dynamic library.[8,28] Gaining control over sorting to enable inclusion of more than one ligand within a metal–organic structure can however be challenging as narcissistic associations often dominate.[27–30] For heteroditopic ligands orientation of the ligand with respect to the metal centre can be governed using steric and electronic arguments to bias either narcissistic or integrative sorting.[11,14,31]

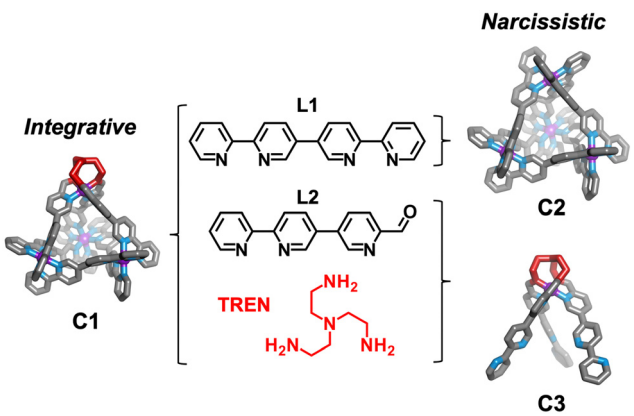

Scheme 1 Left: Self-assembly of a heteroleptic tetrahedral cage **C1** by integrative sorting. Right: Formation of homoleptic cage **C2** and the mononuclear complex **C3**. Exclusive formation of **C1** or social sorting is possible when using **L1**, **L2**, TREN and Fe(II) starting materials.

Department of Chemistry, University of Manchester, Oxford Road, Manchester, M13 9PL, UK. E-mail: imogen.riddell@manchester.ac.uk

† Electronic supplementary information (ESI) available. CCDC 2112326, 2112327, 2112329 and 2112640. For ESI and crystallographic data in CIF or other electronic format see DOI: https://doi.org/10.1039/d2cc04624e

Open Access Article. Published on 18 2022. Downloaded on 2.10.2024 . 19:22:38.
This article is licensed under a Creative Commons Attribution 3.0 Unported Licence.

Herein we detail self-assembly reactions incorporating two similar ligands (Scheme 1; **L1** and **L2**) with a choice of amine and iron(II) salt. The system is shown to display integrative sorting generating **C1** exclusively when TREN and iron perchlorate are employed in the self-assembly reaction. Alternatively, social sorting to form a mixture of two tetrahedral cages **C1** and **C2**, and the mononuclear complex **C3**, is observed when iron triflimide is used in place of iron perchlorate.

The bisbidentate ligands **L1** and **L2** both bind octahedral metal ions through their bidentate N^N binding sites. Ligand 1 (**L1**) contains two bipyridine binding sites and was previously reported to form $[M^{n+}{}_4\mathbf{L1}_6]^{4n+}$ tetrahedral architectures in the presence of octahedrally coordinating metal ions including Fe(II)[32] and Co(III).[33] Ligand 2 (**L2**) features a bidentate bipyridyl binding site at one end and a pyridine aldehyde moiety capable of reacting with a range of amines to generate a bidentate pyridylimine at the other.[34] The relative orientation of the bidentate binding sites in these ligands is comparable, leading us to hypothesis the ligands could be interchanged within $[M_4L_6]^{8+}$ tetrahedra.

To the best of our knowledge, the Fe_4L_6 tetrahedron (**C1**), which incorporates both **L1** and **L2**, is the only example of an M_4L_6 tetrahedron formed through integrative sorting behaviour. Incorporation of **L1** and **L2** generates a structure which has overall C_3-symmetry and incorporates one unique vertex which may allow for introduction of functionality not possible at the *tris*(bipyridine) sites,[35] or affect host guest binding through alteration of guest access and egress.[36]

In initial studies **L1**, **L2**, $Fe(ClO_4)_2$ and the monoamine *p*-toluidine were combined in CD_3CN to determine if the system displayed any self-sorting behaviour. Analysis of the ^{1}H NMR from this reaction showed major peaks corresponding to the homoleptic cage, **C2**, alongside a broad baseline. Mass spectrometric analysis supported the formation of a library of M_4L_6 tetrahedra with between three and six **L1** ligands incorporated (Fig. S5, ESI†). No evidence for formation of cages with greater than three equivalents of **L2** was found suggesting that under the conditions of ionisation cages incorporating significant numbers of this component are less stable.

We next added one equivalent of TREN (T; *tris*(2-aminoethyl)amine) per four metal centres to the library generated with *p*-toluidine, hypothesising that the triamine would displace three equivalents of *p*-toluidine and orientate three pyridyl imines around one metal centre (Fig. 1). Analysis of the ^{1}H NMR spectrum following addition of TREN (Fig S4, ESI†) indicated formation of a single set of resonances corresponding to **C1**, in addition to those of the liberated *p*-toluidine. Single crystals of **C1** (Fig. 2) were grown through slow diffusion of diethyl ether into acetonitrile over the course of seven days. Measurement of the Fe(II) to N bond lengths in the crystal structure of **C1** did not indicate any significant bond strain. All bond lengths were consistent with coordination of low-spin Fe(II) within a N^6 coordination environment. Moreover, these values were comparable with those obtained from the single crystal structure of homoleptic tetrahedron **C2** (Fig. S32, ESI†).

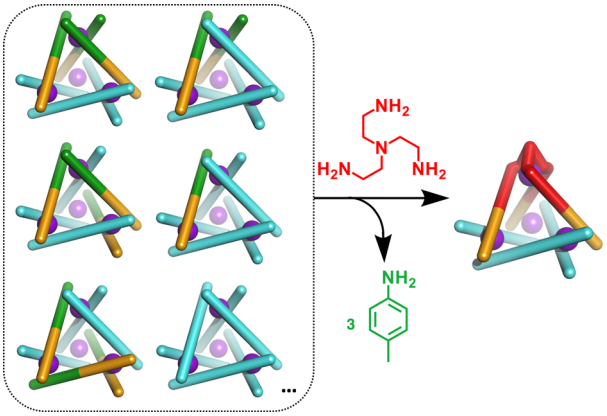

Fig. 1 Displacement of *p*-toluidine (3 equiv.) by TREN(red) to generate **C1** exclusively from a library of cages. The initial library includes a mixture of cages with varying numbers and orientations of **L1** and **L2**.

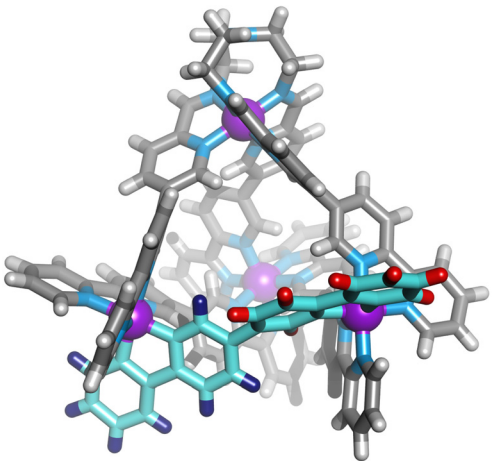

Fig. 2 Single crystal X-ray structure of the cationic portion of **C1**. The two different bipyridine environments on **L1** are coloured blue and red. Counterions and solvent removed for clarity.

Assignment of the ^{1}H NMR spectrum revealed that upon incorporation in **C1**, the two adjacent bipyridine units of **L1** became inequivalent, consistent with formation of the C_3-symmetric tetrahedral architecture (Fig. 2). Refinement of the single crystal X-ray data did not provide definitive evidence for encapsulation of the perchlorate counterion, however, structurally related M_4L_6 tetrahedra have been reported to bind perchlorate anions with high affinity.[33,37]

To try and better understand the factors governing the *p*-toluidine to TREN amine exchange process we next added three equivalents of 2-pyridinecarboxaldehyde and one equivalent of TREN per Fe(II) ion to a solution of purified **C2** constituted from **L1** and Fe(II). After heating the mixture at 65 °C for 24 hours the ^{1}H NMR spectrum contained no evidence of **C2** (Fig. S22, ESI†). Analysis of the reaction mixture confirmed exclusive formation of a mononuclear *tris*pyridylimine complex, and the displaced **L1** ligand precipitated from solution following decomplexation. We therefore propose that

 This journal is © The Royal Society of Chemistry 2022

Open Access Article. Published on 18 2022. Downloaded on 2.10.2024 . 19:22:38.
This article is licensed under a Creative Commons Attribution 3.0 Unported Licence.

displacement of *p*-toluidine from complexes within the library is not the sole driving force for the structural rearrangement observed upon addition of TREN. Demetallation of the M_4L_6 structures, driven by the addition of TREN, also plays a significant role in the structural rearrangement of the mixture. This is consistent with previously reported mechanistic studies.[30]

Next we evaluated the effect the perchlorate counterion had on the ^{1}H NMR profile of the self-assembly reaction mixture. When iron(II) triflimide (4 equiv.) was used in the self-assembly reaction alongside three equivalents of **L1** and **L2** and one equivalent of TREN a complex ^{1}H NMR spectrum was recorded which could not be simplified through common purification techniques. Analysis of the spectrum identified two distinct sets of peaks corresponding to the heteroleptic and homoleptic tetrahedra (**C1** and **C2**, Fig. S20, ESI†). Mass spectroscopic analysis of the reaction mixture also indicated the presence of the mononuclear species **C3** (Fig. S21, ESI†). The large size of the triflimide anion[37] ensures it cannot act as an internal template for either **C1** or **C2** and thus enabled the formation of a mixture of cages in a 1 : 2 **C1** : **C2** ratio. Subsequent addition of potassium perchlorate to the crude mixture of **C1**, **C2** and **C3** synthesised with $Fe(NTf_2)_2$ revealed changes in the ^{1}H NMR spectrum of the mixture that were consistent with encapsulation of this anion within both cages (**C1** and **C2**). The observation that **C1** and **C2** are both capable of binding perchlorate anions is not unexpected given their structural similarities. Both complexes have comparable average Fe-Fe distances (9.36(0.007) Å and 9.44(0.050) Å, respectively) and enclose similarly shaped void cavities of comparable volume (ESI,† S3).

Inspection of the crystal lattice of **C3** with each counterion indicated that the perchlorate ion sits in the C_3-axis at the centre of the threefold symmetric metalloligand, while in the case of NTf_2^- this site is occupied by an acetonitrile molecule. The exclusive formation of **C1** when synthesised from $Fe(ClO_4)_2$ starting materials is thus a kinetic effect, with the metal counterion identified as the discriminating factor in the self-assembly process. Additional studies with BF_4^-, OTf^-, SbF_6^-, AsF_6^-, PF_6^- and ReO_4^- all generated socially sorted mixtures of products incorporating **C1**, **C2** and **C3** (ESI,† S1.3.6), indicating the preferential role of perchlorate in the formation of **C1**.

The formation and structural characterisation of an integratively sorted $M_4(\mathbf{L1})_3(\mathbf{L2})_3T$ metal–organic tetrahedral architecture is reported. M_4L_6 complexes are well documented to have desirable functional properties but, to date, examples of reduced-symmetry tetrahedra are rare. Moreover, formation of M_4L_6 tetrahedra which incorporate more than one ligand or metal ion have all previously been reported as components of statistical libraries. Here we show for the first-time exclusive formation of an integratively sorted M_4L_6 tetrahedron.

The heteroleptic tetrahedron is synthesized through addition of $Fe(ClO_4)_2$ into a system containing subcomponents **L1**, **L2** and TREN. Replacing either iron(II) perchlorate or TREN generated mixtures of products. Understanding the parameters that govern the exclusive formation of **C1** will enable the rational design of non-*T*-symmetric tetrahedra that incorporate dissimilar metal coordination sites. Such structures have increased functionality compared with their symmetric counterparts and present exciting possibilities for further development of metal–organic cages with applications ranging from separation to storage and catalysis.

This research was supported by a Royal Society University Research Fellowship (IAR), the Engineering and Physical Sciences Research Council (grants EP/K039547/1 and EP/R00482X/1), and the Diamond Light Source for the allocated time on the beamline I19 (Cy23480).

Data associated with this article, including experimental procedures, compound characterisation, X-ray crystallography and VOIDOO calculations are available in the ESI.†

I. A. R. conceived and supervised the project; L. L. K. T. designed and performed the experiments and characterised the compounds; R. A. performed experiments and characterised compounds; A. C. Y. S. synthesized novel ligand **L2**; I. J. Y. R. performed all crystallographic characterisation.

Conflicts of interest

There are no conflicts to declare.

Notes and references

1 M. Frank, L. Krause, R. Herbst-Irmer, D. Stalke and G. H. Clever, *Dalton Trans.*, 2014, **43**, 4587–4592.
2 M. Lal Saha and M. Schmittel, *Org. Biomol. Chem.*, 2012, **10**, 4651–4684.
3 F. Crick and J. Watson, *Nature*, 1953, **171**, 737–738.
4 R. H. Carlson, C. V. Gabel, S. S. Chan, R. H. Austin, J. P. Brody and J. W. Winkelman, *Phys. Rev. Lett.*, 1997, **79**, 2149–2152.
5 S. Ackerman, *Discovering the Brain*, National Academies Press (US), Washington (DC), 1992.
6 M. M. Safont-Sempere, G. Fernández and F. Würthner, *Chem. Rev.*, 2011, **111**, 5784–5814.
7 Z. He, W. Jiang and C. A. Schalley, *Chem. Soc. Rev.*, 2015, **44**, 779–789.
8 W. M. Bloch and G. H. Clever, *Chem. Commun.*, 2017, **53**, 8506–8516.
9 S. Pullen, J. Tessarolo and G. H. Clever, *Chem. Sci.*, 2021, **12**, 7269–7293.
10 M. Konopka, P. Cecot, J. M. Harrowfield and A. R. Stefankiewicz, *J. Mater. Chem. C*, 2021, **9**, 7607–7614.
11 M. M. J. Smulders, A. Jiménez and J. R. Nitschke, *Angew. Chem., Int. Ed.*, 2012, **51**, 6681–6685.
12 J. F. Ayme and J. M. Lehn, *Chem. Sci.*, 2020, **11**, 1114–1121.
13 S. Cardona-Serra, E. Coronado, P. Gaviña, J. Ponce and S. Tatay, *Chem. Commun.*, 2011, **47**, 8235–8237.
14 J. E. M. Lewis, A. Tarzia, A. J. P. White and K. E. Jelfs, *Chem. Sci.*, 2020, **11**, 677–683.
15 A. D. Faulkner, R. A. Kaner, Q. M. A. Abdallah, G. Clarkson, D. J. Fox, P. Gurnani, S. E. Howson, R. M. Phillips, D. I. Roper, D. H. Simpson and P. Scott, *Nat. Chem.*, 2014, **6**, 797–803.
16 J. E. M. Lewis and J. D. Crowley, *ChemPlusChem*, 2020, **85**, 815–827.
17 H. Ube, K. Endo, H. Sato and M. Shionoya, *J. Am. Chem. Soc.*, 2019, **141**, 10384–10389.
18 Y. Q. Zou, D. Zhang, T. K. Ronson, A. Tarzia, Z. Lu, K. E. Jelfs and J. R. Nitschke, *J. Am. Chem. Soc.*, 2021, **143**, 9009–9015.
19 J. Tessarolo, H. Lee, E. Sakuda, K. Umakoshi and G. H. Clever, *J. Am. Chem. Soc.*, 2021, **143**, 6339–6344.
20 A. W. Markwell-Heys, M. L. Schneider, J. M. L. Madridejos, G. F. Metha and W. M. Bloch, *Chem. Commun.*, 2021, **57**, 2915–2918.
21 T. K. Ronson, D. A. Roberts, S. P. Black and J. R. Nitschke, *J. Am. Chem. Soc.*, 2015, **137**, 14502–14512.
22 M. M. J. Smulders, I. A. Riddell, C. Browne and J. R. Nitschke, *Chem. Soc. Rev.*, 2013, **42**, 1728–1754.

Open Access Article. Published on 18 2022. Downloaded on 2.10.2024 . 19:22:38.
This article is licensed under a Creative Commons Attribution 3.0 Unported Licence.

23 A. J. Metherell and M. D. Ward, *Chem. Sci.*, 2016, **7**, 910–915.
24 Q. F. Sun, S. Sato and M. Fujita, *Angew. Chem., Int. Ed.*, 2014, **53**, 13510–13513.
25 A. Wu and L. Isaacs, *J. Am. Chem. Soc.*, 2003, **125**, 4831–4835.
26 F. J. Rizzuto and J. R. Nitschke, *J. Am. Chem. Soc.*, 2020, **142**, 7749–7753.
27 L. R. Holloway, P. M. Bogie and R. J. Hooley, *Dalton Trans.*, 2017, **46**, 14719–14723.
28 L. R. Holloway, Narcissistic Self-Sorting, Reactivity and Post-Assembly Modifications of Metal-Ligand Cage Complexes, UC Riverside, California, United States of America, 2018, **https://escholarship.org/uc/item/6bw2b9gg**.
29 X. Zhao, H. Wang, B. Li, B. Zheng, D. Yang, W. Xu, X. Li, X. J. Yang and B. Wu, *Chem. Commun.*, 2021, **57**, 6078–6081.
30 L. R. Holloway, M. C. Young, G. J. O. Beran and R. J. Hooley, *Chem. Sci.*, 2015, **6**, 4801–4806.
31 K. Mahata, M. L. Saha and M. Schmittel, *J. Am. Chem. Soc.*, 2010, **132**, 15933–15935.
32 C. R. K. Glasson, J. K. Clegg, J. C. McMurtrie, G. V. Meehan, L. F. Lindoy, C. A. Motti, B. Moubaraki, K. S. Murray and J. D. Cashion, *Chem. Sci.*, 2011, **2**, 540–543.
33 B. P. Burke, W. Grantham, M. J. Burke, G. S. Nichol, D. Roberts, I. Renard, R. Hargreaves, C. Cawthorne, S. J. Archibald and P. J. Lusby, *J. Am. Chem. Soc.*, 2018, **140**, 16877–16881.
34 M. L. Saha, S. Neogi and M. Schmittel, *Dalton Trans.*, 2014, **43**, 3815–3834.
35 S. L. Han, J. Yang, D. Tripathy, X. Q. Guo, S. J. Hu, X. Z. Li, L. X. Cai, L. P. Zhou and Q. F. Sun, *Inorg. Chem.*, 2020, **59**, 14023–14030.
36 L. Zhang, Y. Jin, G. H. Tao, Y. Gong, Y. Hu, L. He and W. Zhang, *Angew. Chem., Int. Ed.*, 2020, **59**, 20846–20851.
37 I. A. Riddell, Y. R. Hristova, J. K. Clegg, C. S. Wood, B. Breiner and J. R. Nitschke, *J. Am. Chem. Soc.*, 2013, **135**, 2723–2733.

 This journal is © The Royal Society of Chemistry 2022